Scalable Computing: Practice and Experience, ISSN 1895-1767, http://www.scpe.org
© 2024 SCPE. Volume 25, Issues 4, pp. 2532–2539, DOI 10.12694/scpe.v25i4.2825

FILM AND TELEVISION SPECIAL EFFECTS AI SYSTEM INTEGRATING COMPUTER ARTIFICIAL INTELLIGENCE AND BIG DATA TECHNOLOGY

YAO JU*AND GUOBIN WEI†

Abstract. Particle systems can achieve many scenarios that are difficult to achieve in the field or expensive in reality. In this paper, the requirements of 3D film special effects and the design process of particle systems are studied. Unity3D engine was used to simulate 3D movie special effects. Then, the motion trajectory planning of 3D video group animation characters based on particle swarm optimization is proposed. Then, the system models the animated characters' moving track to achieve the realism's dynamic effect. This project intends to use the gravity optimization method for particle swarm optimization. The aim is to overcome the optimization difficulty caused by particle swarm optimization, which is easy to fall into local extreme values. Finally, the generated trajectory information is input into the 3D simulation system for conflict detection and clustering tests. Experiments show that the proposed algorithm can effectively render memorable scenes such as movies and TV. The picture has a high real-time frame rate and is realistic.

Key words: Film and television; Special effects animation; Particle system; 3D special effects; Particle swarm optimization; Collision avoidance

1. Introduction. 3D special effects have been widely used in science fiction, martial arts, animation and other movies and TV series, and it has gradually developed into a significant sign to measure the visual quality of contemporary film and television works. For example, "Transformers 3", "Men in Black 3", "The Day after Tomorrow," and so on use particle technology to achieve three-dimensional special effects such as explosions, building collapses, fireworks and so on. The production team will integrate the three-dimensional film effect with the natural theme scene, which can not only fully mobilize the creative passion of the producer but also save a lot of production costs. Secondly, many memorable scenes are complex to be photographed in actual situations, which may also be because such scenes do not exist in reality. For example, human cell division, the process of seasonal changes in trees and flowers, is challenging to photograph in the same time and space. Real effects waves crashing into cities, volcanoes erupting, buildings exploding, smoke, etc., are costly. Particles are 2D images generated in 3D and then repeatedly drawn with various materials to create a 3D movie effect. Using particle systems to simulate memorable scenes that are impossible to achieve in reality is an integral part of the research and development of movies and television programs.

Reference [1] uses a fast simulated annealing algorithm based on hybrid particle swarm optimization. A model for solving high-dimensional optimal problems is presented. The particle swarm optimization algorithm determines the global optimization range, and FSM is used to refine the optimization range. Reference [2] A method integrating particle swarm optimization algorithm (PSO) and genetic algorithm (GA) is proposed to improve the adaptability of the system based on reference [1]. Given the problems in the current population evolution, such as complex coordination of local search ability and easy falling into local extreme values, SUANFA was improved using particle swarm technology in literature [3]. In this way, the algorithm model has fast convergence speed, high precision and strong robustness. In literature [4], an adaptive neural network algorithm based on weights was designed to solve problems such as low optimization accuracy and "premature convergence" in practical applications. Literature [5] studies the group behavior simulation method aiming at generating and propagating fear emotion under multiple disaster scenarios.

Unity3D is a 3D game engine. It supports Windows, MacOS desktop operating system platforms and mobile operating system platforms like Android and iOS. It includes graphics, sound, physical, network, particles and

*Anhui University of Finance and Economics, Bengbu, Anhui 233030, China (xyjuyao@163.com)
†Anhui University of Finance and Economics, Bengbu, Anhui 233030, China

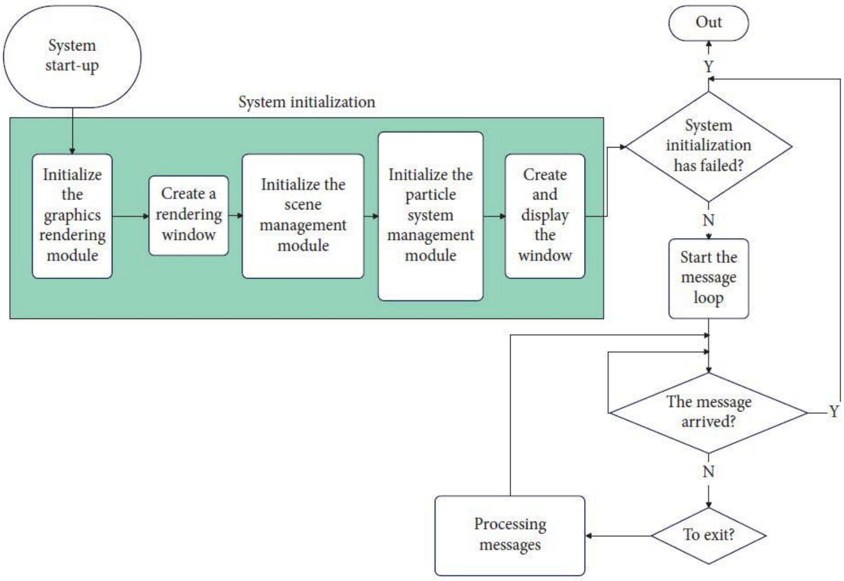

Fig. 2.1: *3D visual effects development process of the particle system.*

other functional components [6]. It uses scripting languages such as C# and JavaScript and can support most 3D model documents. The platform has a variety of light rendering systems such as soft shadow, baking and powerful graphics editing functions. This method can be used to simulate large-scale virtual environments and develop 3D online games. It can also realize the simulation of digital 3D movie effects such as smoke, smoke, flame, smoke, lightning, explosion, etc. This paper studies the requirements of 3D film special effects and the particle system design process. Unity3D engine was used to simulate 3D movie special effects [7]. Then, the motion trajectory planning of 3D video group animation characters based on particle swarm optimization is proposed. Then, the system models the animated characters' moving track to achieve a realistic dynamic effect.

2. Introduction to particle systems. Reeves et al. introduced the particle system 1983, which can simulate targets of any shape, such as smoke, waves, water currents, flames, rain and snow, clouds, explosions, forests, etc. Because the particles in the particle system have the characteristics of shape, size, color, transparency, moving speed, moving direction, life, etc., and have the characteristics of spatiotemporal dynamic distribution, it can simulate the motion effects of various motion rules [8]. Particle systems can simulate complex and varied objects or scenes in various shapes. According to the particle shape, it can be divided into fluid particles, smoke particles and broken particles. Flow particles are primarily used to simulate special effects such as water flow, wave, flame and magma. Smoke particles are dynamic particle effects [9]. It grows and dies over time. Pulverized particles are used to simulate the action of matter in the explosion process, usually accompanied by the formation of explosive fragments of matter. Figure 2.1 shows the development process of 3D visual effects for particle systems (figure cited in Scientific Programming, 2022, 202:1-11.).

3. Improved particle swarm optimization algorithm for 3D animation group trajectory optimization.

3.1. Key Issues. Group behavior requires not only the randomness of movement trajectories but also the global consistency. Only in this way can we produce actual group intelligence animation. To this end, this project will carry out research from the following aspects: (1) Each individual in the cluster has its scope of activity to prevent conflicts effectively. (2) The population is a whole. All the individuals in the population move in the same direction or for the same purpose. (3) The population can be divided into several smaller populations. According to certain conditions, it can form a large population by itself. (4) Enhanced track authenticity. The individual's movement path not only has independence but also guarantees the unity of the whole, which conforms to the law of group movement. (5) Improving the coordination ability of the population. It enhances the intelligence of the cluster and speeds up the movement rate of the cluster.

3.2. Particle swarm optimization algorithm . Suppose the search space is N and all the particles sum is n. The PSO algorithm is explained by formula (3.1) and formula (3.2)

$$u_1(k+1) = u_1(k) + \varepsilon_1 \times \omega() \times [Q_2(k) - x_1(k)] + \varepsilon_2 \times \omega() \times [Q_3(k) - x_1(t)] \tag{3.1}$$

$$x_1(k+1) = x_1(k) + u_1(k+1) \tag{3.2}$$

In formula $1 \leq i \leq n, 1 \leq d \leq N. u_i(k)$ represents the speed of the i particle at the k iteration, and $x_i(k)$ represents the position of the i particle at the k iteration. d represents the size of particle $i.Q_2$ represents the optimal particle distribution and Q_3 represents the optimal location of the population of the i particle. ε_1 and ε_2 are positive values of the acceleration coefficient. $\omega()$ stands for any number from 0 to 1 .

3.3. Improved particle swarm optimization to solve the path planning of $3^{\mathbf{D}}$ animation . Although the particle swarm optimization algorithm has many advantages, it is easy to enter the minimum point, which reduces the optimization accuracy [10]. In this project, gravity optimization (GSA) and particle swarm (PSO) technology are organically integrated to overcome the disadvantage that PSO can easily fall into local extreme values. In this way, the overall optimization ability of PSO is improved. The modified algorithm is determined by the following formula $(3 \cdot 3)$

$$u_i^d(k+1) = \lambda \times u_i^d(k) + \varepsilon_1 \times \omega() \times \delta_i^d(k) + \varepsilon_2 \times \omega() \times \left[H_{\text{best}} - x_i^d(k)\right] \tag{3.3}$$

$u_i^d(k)$ is the rate of particle i at time k in the d iteration. ε_1 and ε_2 are acceleration factors. Where λ is an inert component. $\omega()$ is any number in the interval $[0,1].\delta_i^d(k)$ is the acceleration of the particle i at time k in the d iteration. H_{bst} represents the best solution so far. Formula (3.4) is used to update theladaptive weighting to improve its search performance

$$\lambda = \lambda_{\max} - (\lambda_{\max} - \lambda_{\min}) \times \frac{g_{\text{clovert}} - g_{\text{worst}}}{g_{\text{best}} - g_{\text{worst}}} \tag{3.4}$$

g_{croren} stands for the current fitness function. g_{best} represents the optimal fitness of the particle. g_{worst} represents the worst fitness of the particle. This project intends to incorporate the natural characteristics of bird clusters into the method to improve its complexity and search range without local optimal solutions [11]. The new position of the agent after each repetition is updated according to formula (3.5)

$$x_i^d(k+1) = x_i^d(k) \tag{3.5}$$

In the later iteration process, the genetic variation of the genetic algorithm will gradually weaken so it can quickly enter the local extreme value. So, look carefully at the H_{best} value after each cycle. If the H_{best} fitness remains constant after several iterations, the particle is in A suboptimal state. The local movement process is then started to avoid stalling. This paper calls it global response [12]. The individual particles can be updated using formula (3.6) to explore a more extensive range of sites

$$\hat{x}_k = \overset{\mathrm{r}}{x}_k + \omega_1 \left(\frac{1}{6} \sum_{n \in N_i}^{\overset{\mathrm{r}}{x}_n} \right) (3.6) \tag{3.6}$$

$\hat{x}_k$ is the new position after the overall response to $\hat{x}_k$. The new positioning is determined by averaging the six closest points. Set N_i has an exponent of 6 adjacent particles $\overset{1}{x}_k$.

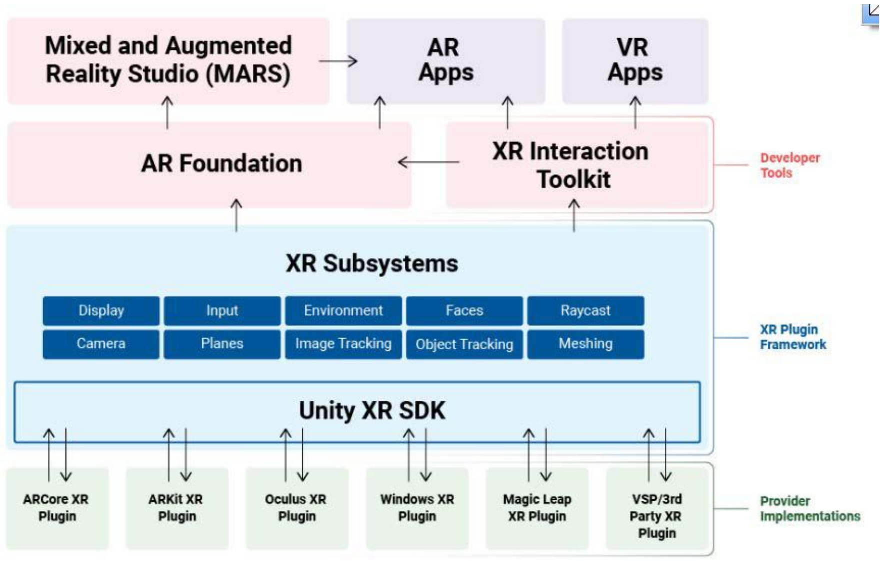

Fig. 4.1: *The overall structure of the special effects animation-assisted generation system.*

4. Realization of three-dimensional film and television special effects based on Unity3D technology . Particle animation in Unity3D comprises three components: particle generator and particle animator. A simple stationary particle system can be constructed using a particle generator and rendering method [13]. When the particle system interacts with other virtual objects, a particle impact device can be added to the object. In Unity3D, particle emitters are divided into ellipsoid and network structures. Ellipsoidal particle emitters can form a series of spheroidal regions of particles. The ellipsoidal characteristics are used to scale and expand the sphere. Particle generators generate particles from the surface of the grid and emit them around the grid. The software can move at multiple angles according to particle characteristics [14]. At the same time, the system can operate each particle to make it have more abundant effects. The particle rendering machine presents the graphics generated by the particle system on the display screen so the user can see the corresponding graphics directly. They are using particle collisions to interact with other objects. For example, it can achieve an explosive effect when the object is in contact with the explosive object. The overall structure of the special effects animation-assisted generation system is shown in Figure 4.1. The system is divided into three modules: front-end browser, back-end server and communication network. The front-end browsing subsystem can play, pause and stop the animation of movie special effects. In the display interface, the user can input the effect text of the animation and movie that he wants to make on the display screen. The system produces the effect of the movie according to the user's input [15]. The system uses a communication network to transfer information between the front browsing subsystem and the back terminal system, including database, text analysis, animation production, special effects production, and the other five modules. The system includes animation features and animation instructions. It can store a large number of anime and movie special effects materials. In the text analysis part, fuzzy semantic analysis is used to analyze the text and generate the corresponding animation. The film effect generation module uses particle technology to produce the film effect. The wavelet transform theory is applied to combine the animation and film effects produced by the system [16]. Through the communication network, the synthesized film special effects animation is transmitted to the front-end browsing subsystem to achieve the purpose of human-machine dialogue with users.

5. System inspection .

5.1. Experimental Detection. Select Windows 2010 operating system, Core i9 9100 processor, 8 GB memory as hardware configuration. Visual Studio 2018 and OGRE image engine were used to verify the designed system [17]. Two different database structures, MySQLServer5.0 and MySQL dB, are adopted. The

Table 5.1: Comparison results of collision detection.

Action name	Text system	Bounding box system	STM system
Displacement action	89	165	200
Joint action	79	169	191
Leg action	96	143	183
Hand movement	84	155	175
Rotating action	81	175	181
Jumping action	90	161	190
squat	95	180	160
brandishing	82	172	194

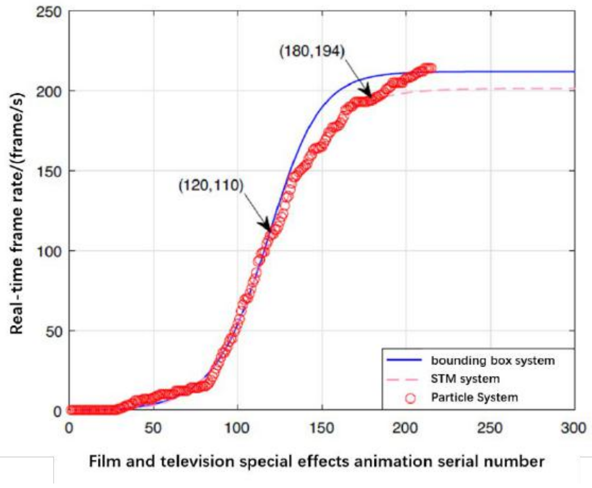

Fig. 5.1: *Real-time frame rate comparison of different systems.*

test results shown in Table 5.1 are compared with the closed frame and STM methods.

The conflict detection results in Table 5.1 show the conflicts between various behaviors when generating dynamic images. Compared with the scanning tunnel model, the conflict detection algorithm of this method is significantly reduced. The simulation results show that this method is fast and can meet the needs of a fast generation of film special effects animation [18]. This system helps to generate the actual time frame rate of 10 movie special effects animations. This system must meet 30 frames per second of video. At this time, the fluency of the film effect can be guaranteed. The wraparound and STM systems were selected to compare real-time frame rates (Figure 5.1). From the real-time frame rate comparison in FIG. 5.1, it can be seen that all three algorithms can achieve a speed of 30 frames/SEC. The real-time frame rate of PSO in this paper is much higher than that of the other two algorithms. The test proves that the designed software can meet the real-time processing requirements. It can be used for automatic synthesis of film animation effects.

The software of this paper is used to calculate ten different types of movie effects and compare them with the bounding box system and STM system. The results of the comparison are shown in Table 5.2.

The data in Table 5.2 shows that the number of vertices of movie special effects animation assisted by the software in this paper is more than that of the bounding box system and the STM system. This proves our software is more realistic and livelier than the other two systems [19]. It shows that the system in this paper has better assist in generating special effects animation.

5.2. Special Effects Detection. Add the rain instance system rain, which consists of an ellipsoid particle emitter, particle animator, particle renderer, particle collider, sound source and other components. The paper

Special effects animation serial number	Text system	
	Number of vertices	Face number
1	16081	13913
2	15878	14851
3	18295	16397
4	20151	19221
5	19234	17577
6	15934	14852
7	18183	16931
8	18806	17954
9	19442	18590
10	17176	16015
Special effects animation serial number	Bounding box system	
	Number of vertices	Face number
1	13069	10681
2	12003	13981
3	12871	11947
4	14043	13172
5	13596	12988
6	13901	12970
7	12560	12290
8	12346	10886
9	13175	11945
10	13410	12450
Special effects animation serial number	STM system	
	Number of vertices	Face number
1	14088	12931
2	13064	12452
3	14028	13511
4	14424	12138
5	14217	13202
6	13525	13376
7	12225	11297
8	13172	12049
9	14026	13331
10	13602	13277

Table 5.2: *Statistics of numerical comparison of special effects of film and television special effects.*

added rain and snow sound files to the sound source component to make rain and snow even better. Then, two-particle systems were built initially to simulate the wave and spray effects [20]. At the same time, text was added to the particle system to mimic the rippling and splashing effect of rain hitting the land. By controlling characteristic parameters such as texture mapping, particle size and particle emission velocity of the particle system, simulation of various rain and snow effects can be easily achieved (Figs. 5.2 and 5.3).

5.2. Special Effects Detection. 3D movie effects can mimic natural phenomena. It solves the difficulty of scene shooting and the time and space limitation of life growth. Swarm motion in 3D animation is studied by using a particle swarm optimization algorithm. A particle swarm optimization algorithm based on cluster behavior and gravity optimization is studied to overcome the optimization difficulty caused by local extreme values in PSO. Secondly, a solution strategy based on conflict detection and collision avoidance is studied. Finally, the obtained trajectory information is input into the 3D simulation platform and conflict and clustering tests are carried out. The results show that this system can satisfy the realistic sense of special effects animation. At the same time, its real-time expressiveness and flexibility can meet the system's requirements. The system

Fig. 5.2: *3D dynamic rain effects.*

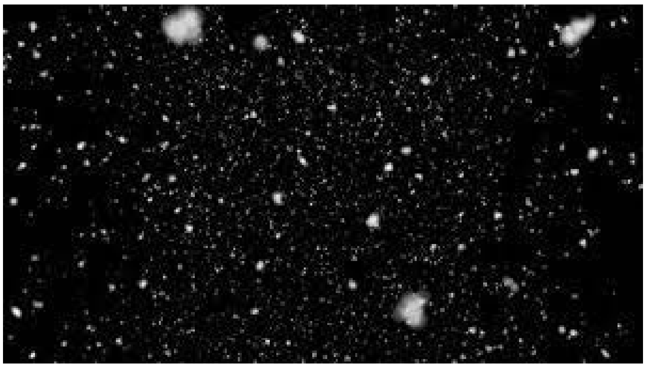

Fig. 5.3: *3D visual effects development process of the particle system.*

can make the movie's special effects animation more vivid and lifelike.

REFERENCES

[1] Droguet, B. E., Liang, H. L., Frka-Petesic, B., Parker, R. M., De Volder, M. F., Baumberg, J. J., & Vignolini, S. (2022). Large-scale fabrication of structurally coloured cellulose nanocrystal films and effect pigments. Nature materials, 21(3), 352-358.

[2] Lisuzzo, L., Caruso, M. R., Cavallaro, G., Milioto, S., & Lazzara, G. (2021). Hydroxypropyl cellulose films filled with halloysite nanotubes/wax hybrid microspheres. Industrial & Engineering Chemistry Research, 60(4), 1656-1665.

[3] Wu, X., Toe, C. Y., Su, C., Ng, Y. H., Amal, R., & Scott, J. (2020). Preparation of Bi-based photocatalysts in the form of powdered particles and thin films: a review. Journal of Materials Chemistry A, 8(31), 15302-15318.

[4] Cui, Y., Duan, W., Jin, Y., Wo, F., Xi, F., & Wu, J. (2020). Ratiometric fluorescent nanohybrid for noninvasive and visual monitoring of sweat glucose. ACS sensors, 5(7), 2096-2105.

[5] Franklin, D., He, Z., Mastranzo Ortega, P., Safaei, A., Cencillo-Abad, P., Wu, S. T., & Chanda, D. (2020). Self-assembled plasmonics for angle-independent structural color displays with actively addressed black states. Proceedings of the National Academy of Sciences, 117(24), 13350-13358.

[6] Kim, I., Viswanathan, K., Kasi, G., Thanakkasaranee, S., Sadeghi, K., & Seo, J. (2022). ZnO nanostructures in active antibacterial food packaging: Preparation methods, antimicrobial mechanisms, safety issues, future prospects, and challenges. Food Reviews International, 38(4), 537-565.

[7] Tegunov, D., Xue, L., Dienemann, C., Cramer, P., & Mahamid, J. (2021). Multi-particle cryo-EM refinement with M visualizes ribosome-antibiotic complex at 3.5 Å in cells. Nature Methods, 18(2), 186-193.

[8] Hebner, T. S., & Maurer-Jones, M. A. (2020). Characterizing microplastic size and morphology of photodegraded polymers placed in simulated moving water conditions. Environmental Science: Processes & Impacts, 22(2), 398-407.

[9] Gerashi, E., Alizadeh, R., & Langdon, T. G. (2022). Effect of crystallographic texture and twinning on the corrosion behavior of Mg alloys: A review. Journal of Magnesium and Alloys, 10(2), 313-325.

[10] Li, Y., Diddens, C., Segers, T., Wijshoff, H., Versluis, M., & Lohse, D. (2020). Evaporating droplets on oil-wetted surfaces: Suppression of the coffee-stain effect. Proceedings of the National Academy of Sciences, 117(29), 16756-16763.
[11] Zhang, J., Zhang, L., & Gong, X. (2021). Large-scale spraying fabrication of robust fluorine-free superhydrophobic coatings based on dual-sized silica particles for effective antipollution and strong buoyancy. Langmuir, 37(19), 6042-6051.
[12] Ortiz, D. G., Pochat-Bohatier, C., Cambedouzou, J., Bechelany, M., & Miele, P. (2020). Current trends in Pickering emulsions: Particle morphology and applications. Engineering, 6(4), 468-482.
[13] Jacucci, G., Vignolini, S., & Schertel, L. (2020). The limitations of extending nature's color palette in correlated, disordered systems. Proceedings of the National Academy of Sciences, 117(38), 23345-23349.
[14] Shin, J. J., Kim, E. J., Ku, K. H., Lee, Y. J., Hawker, C. J., & Kim, B. J. (2020). 100th anniversary of macromolecular science viewpoint: Block copolymer particles: Tuning shape, interfaces, and morphology. ACS Macro Letters, 9(3), 306-317.
[15] Rey, M., Fernandez-Rodriguez, M. A., Karg, M., Isa, L., & Vogel, N. (2020). Poly-N-isopropylacrylamide nanogels and microgels at fluid interfaces. Accounts of chemical research, 53(2), 414-424.
[16] Buscaglia, V., & Randall, C. A. (2020). Size and scaling effects in barium titanate. An overview. Journal of the European Ceramic Society, 40(11), 3744-3758.
[17] Wu, P., Wang, J., & Jiang, L. (2020). Bio-inspired photonic crystal patterns. Materials Horizons, 7(2), 338-365.
[18] Liu, C., Cheng, Y. B., & Ge, Z. (2020). Understanding of perovskite crystal growth and film formation in scalable deposition processes. Chemical Society Reviews, 49(6), 1653-1687.
[19] Cao, Q., Fan, Q., Chen, Q., Liu, C., Han, X., & Li, L. (2020). Recent advances in manipulation of micro-and nano-objects with magnetic fields at small scales. Materials Horizons, 7(3), 638-666.
[20] Asadi, S., & Pirsa, S. (2020). Production of biodegradable film based on polylactic acid, modified with lycopene pigment and TiO2 and studying its physicochemical properties. Journal of Polymers and the Environment, 28(2), 433-444.

Edited by: Zhigao Zheng
Special issue on: Graph Powered Big Aerospace Data Processing
Received: Nov 9, 2023
Accepted: Nov 24, 2023